

# Mining individual daily commuting patterns of dockless bike-sharing users: a two-layer framework integrating spatiotemporal flow clustering and rule-based decision trees

Caigang Zhuang<sup>a</sup>, Shaoying Li<sup>a</sup>, Xiaoping Liu<sup>b,\*</sup>

<sup>a</sup> School of Geography and Remote Sensing, Guangzhou University, Guangzhou, China

<sup>b</sup> School of Geography and Planning, Sun Yat-sen University, Guangzhou, China

## Abstract

The rise of dockless bike-sharing systems has led to increased interest in using bike-sharing data for urban transportation and travel behavior research. However, few studies have focused on the individual daily mobility patterns, hindering their alignment with the increasingly refined needs of urban active transportation planning. To bridge this gap, this study presents a two-layer framework, integrating improved flow clustering methods and multiple rule-based decision trees, to mine individual cyclists' daily home-work commuting patterns from vast dockless bike-sharing trip data with users' IDs. The effectiveness and applicability of the framework is demonstrated by over 200 million dockless bike-sharing trip records in Shenzhen. Ultimately, based on the mining results, we obtain two categories of bike-sharing commuters (i.e., 74.38% of *Only-biking commuters* and 25.62% of *Biking-with-transit commuters*) and some interesting findings about their daily commuting patterns. For instance, lots of bike-sharing commuters live near urban villages and old communities with lower costs of living, especially in the central city. *Only-biking commuters* have a higher proportion of overtime than *Biking-with-transit commuters*, and the Longhua Industrial Park,

a manufacturing-oriented area, having the longest average working hours (over 10 hours per day). Massive commuters utilize bike-sharing for commuting to work more frequently than for returning home, which is closely related to the over-demand for bike-sharing around workplaces during commuting peak. Overall, this framework offers a cost-effective way to understand residents' non-motorized mobility patterns. Moreover, it paves the way for subsequent research on fine-scale cycling behaviors that consider demographic disparities in socio-economic attributes.

**Keywords:** Dockless Bike-sharing Trip; Spatiotemporal Flow Clustering; Rule-based Decision Trees; Home-work Commuting; Shenzhen

## 1. Introduction

Compared with other modes of mobility, cycling is considered an eco-friendly, healthy, and sustainable mode of transportation, which has a beneficial effect on reducing traffic congestion, energy consumption, and air pollution (DeMaio, 2009; Handy et al., 2014). In the past decade, the spread of the bike-sharing programs has further expanded the benefits of cycling. For example, the convenience of mobile payments and the flexibility of station-less rental services have made dockless bike-sharing, one of the innovative bike-sharing systems, widely accepted and utilized worldwide (Zhang & Mi, 2018; Si et al., 2019). These bike-sharing programs enable cycling to play an essential role in solving the first-and-last-mile trip problem and enhancing urban transport resilience (Fishman, 2016; Cheng et al., 2021; Teixeira et al., 2021). Therefore, how to increase the cycling willingness of residents to promote the development of sustainable and active transportation has received extensive research attention.

In the early years, relevant studies were conducted based on travel survey data which have the limitations of high cost, low timeliness, and small sample size (Li et al., 2021). With the advent of big data era and new bike-sharing systems, the availability of GPS datasets from bike-sharing operators have opened opportunities for cycling-related research. Existing literature has proven that such GPS trajectory data have the advantages of objectivity, high spatiotemporal resolution, and large sample volume (Lu & Liu, 2012). Meanwhile, many scholars have used these data for cycling influence mechanisms analysis (Shen et al., 2018; Ma et al., 2020; Gao et al., 2021a), travel pattern mining (Zhou, 2015; Du et al., 2019; Yao et al., 2019; Cao et al., 2020; Zhang et al., 2021a; Gao et al., 2022), purpose inference (Xing et al., 2020; Li et al., 2021; Ross-Perez et al., 2022), and benefit assessment (Zhang & Mi, 2018; Luo et al., 2019; Gao et al., 2021b). For instance, Shen et al. (2018) explored the factors influencing bike usage based on nine consecutive days of bike-sharing trip records in Singapore, and found that high land use mixtures, easy access to public transportation, and more available cycling facilities are positively correlated with bike-sharing usage. In a study that used a week of bike-sharing data collected in Shenzhen, Li et al. (2021) proposed a framework for inferring the trip purpose of cyclists based on gravity models and Bayesian rules, and revealed the spatiotemporal patterns of nine categories of travel activities. Additionally, Zhang & Mi (2018) extracted bike-sharing usage and trip distances in Shanghai, and estimated the environmental benefits of bike-sharing on emission reduction. These studies are meaningful as they deepen current understanding of the role bike-sharing play in urban transportation and residents' travel behaviors.

However, the aforementioned research based on bike-sharing trip data has rarely focused on the daily travel habits of individual cyclists, despite some leveraging datasets that contain user IDs. To date, the most relevant research has been conducted by a limited number of scholars who attempt to explore the travel characteristics of different user groups, utilizing user attributes information (e.g., age, gender, and membership) available within the docked bike-sharing trip dataset (Zhou, 2015; Yao et al., 2019; Ma et al., 2020). For example, Zhou (2015) constructed bike flow similarity graphs and used community detection techniques to discover the different travel trends for customers and subscribers. Although these studies contributed to understanding the differences in travel patterns within the cycling groups, these methods are not applicable to dockless bike-sharing trip dataset that include little individual attribute information (for privacy concerns). Moreover, the above research merely categorizes cycling user groups based on the similarities in user attributes, rather than extracting daily bicycle mobility patterns at the individual level.

Notably, mining the individual daily mobility patterns of bike-sharing users holds significant implications for the increasingly refined planning of active transportation system (Ferretto et al., 2021). For instance, it can serve as a low-cost, high-coverage technique to complement traditional, expensive, and less comprehensive transportation travel surveys, assisting transportation planners and bike-sharing operators in understanding residents' daily active travel patterns or cycling needs. Furthermore, if bike-sharing users' residential and workplace information can be identified from individual daily mobility patterns, it would enable the integration of various socio-economic data (e.g., housing price) to explore fine-scale studies of cycling behaviors considering population differentiations (Xu et al., 2018;

Wu et al., 2023), thereby providing decision-making basic for the building of human-oriented, bicycle-friendly environments.

So far, there have been some studies proposing methodological frameworks for mining individual daily mobility patterns based on specific geotagged big data, such as cellphone call detail records (CDR) data (Kung et al., 2014; Jiang et al., 2017; Yin et al., 2021), check-in data (Cheng et al., 2011; Li et al., 2013; Wu et al., 2023), and smart card data (Sari Aslam et al., 2019; Zhang et al., 2020). However, these studies' utilized geotagged data do not include any fields related to cycling trips, and thus we cannot identify individual cycling mobility patterns from their mining results. Additionally, due to differences in data features, travel characteristics, and influencing factors, dockless bike-sharing trip data are not suitable as inputs for these frameworks. For example, Jiang et al. (2017) developed an integrated pipeline that can parse, filter, and expand the CDR data to extract human mobility patterns. However, since most bike-sharing trip data only record cycling origins and destinations (ODs), rather than capturing continuous trajectory like CDR data, CDR-based extraction methods are not suitable for bike-sharing data. In a study leveraging Twitter check-in data, Cheng et al. (2011) proposed a recursive grid search method to detect users' homes and subsequently analyze their mobility patterns. Although it is feasible to reconstruct bike-sharing data into check-in-like data by delineating the origin and destination of each trip, this approach results in the loss of key cycling attribute (e.g., trip distance and duration). Thus, using bike-sharing data to check-in-based mining methods can only exploit partial data information. Compared with the geotagged data mentioned above, the features of smart card data are closer to those of bike-sharing data. Recently, several studies have proposed methods

based on such data to extract users' daily activities, such as a heuristic model developed by Sari Aslam et al. (2019) for detecting the residence and workplace of individuals, and a decision tree method presented by Zhang et al. (2020) for identifying the individual stay areas. Nevertheless, noted that the locations of transit stations in the smart card data are fixed, which is significantly different from dockless bike-sharing. Moreover, the travel characteristics and influencing factors of public transport also differ from those of cycling (e.g., shorter trip distances, more affected by weather and etc.). Hence, there are limitations in using the extraction method based on smart card data for dockless bike-sharing data.

In summary, to address the gaps in related studies, this paper will present a two-layer framework that aims to capture the most dominant daily mobility pattern of individual dockless bike-sharing users, i.e., home-work-commuting. Specifically, in Layer 1, we develop flow clustering methods that improved spatiotemporal constraints tailored to the travel characteristics of bike-sharing. This enhancement allows us to derive spatiotemporal flow clusters, effectively representing the daily travel trajectories of individuals, from the biking records that lack geocoding information. However, these trajectories identified in Layer 1 lack semantic information. Therefore, in Layer 2, we further establish rule-based decision trees that incorporate round-trip journeys, working hours, and public transportation transfers for identifying daily commuting trips within individual spatiotemporal flow clusters and dividing bike-sharing users into *Only-biking* and *Biking-with-transit* commuters. To examine the effectiveness and applicability of this two-layer framework, this paper conducts an empirical study using comparative analysis and residence location test in Shenzhen, China, a metropolis with over one million daily bike-sharing trips. Finally, based on the extracted results of individual commuting trips of bike-sharing users, we further analyze their daily

commuting characteristics and spatiotemporal patterns and discuss some meaningful findings and policy implications.

## **2. Study area and dataset**

### *2.1 Study area*

Shenzhen is located in the Guangdong-Hong Kong-Macao Bay Area, which is one of the most densely populated and economically prosperous regions in China. By the end of 2021, Shenzhen has a permanent population of over 17 million and a regional GDP of over 300 billion RMB (Guangdong Statistical Yearbook, 2021). The high-frequency population mobility and booming economic activities are accompanied by huge travel demand. The well-established public transportation systems (11 metro lines and 927 bus lines have been opened as of 2021, Transportation Bureau of Shenzhen, 2021) and shared mobility services (e.g., bike-sharing and ride-sharing) have played an important role in meeting residents' travel needs. Among them, the dockless bike-sharing system was first introduced to Shenzhen in 2016. After the initial period of market dominance and the subsequent period of policy regulation, bike-sharing services have recently been integrated into the daily mobility of local residents. As of July 2022, Shenzhen has over 41,000 dockless bike-sharing with an average of approximately 1.29 million daily trips (Statistics Bureau of Shenzhen, 2022). Usage hotspots are notably in the Futian, Nanshan, Luohu, Bao'an, and Longhua districts (Fig.1), with the extensive bike-sharing trips data offering a rich resource for this paper to mine individual daily cycling commuting patterns.

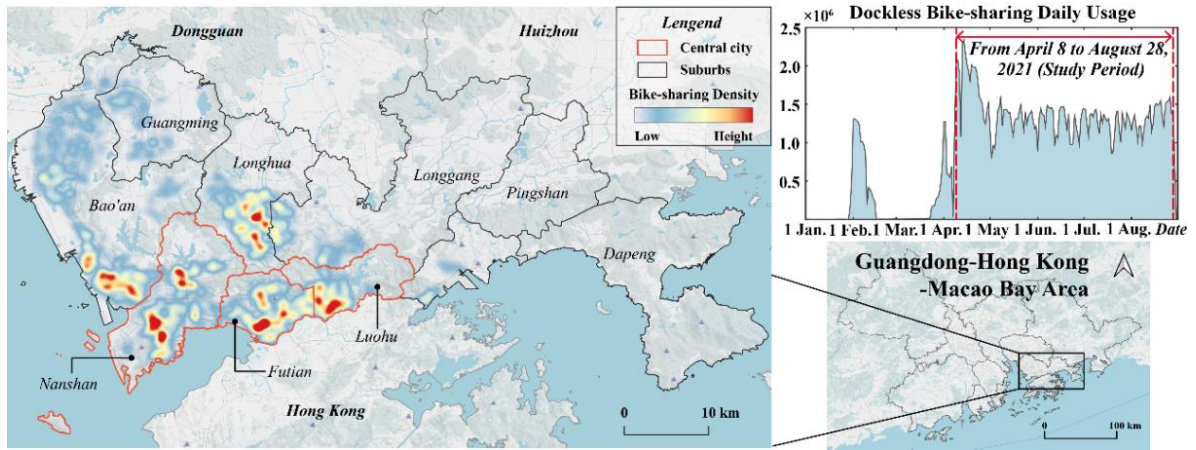


**Fig. 1** Spatial and temporal distribution of raw dockless bike-sharing data in the study area.

## 2.2 Data description

The dockless bike-sharing data used in this study are collected from the Shenzhen government data open platform (<https://opendata.sz.gov.cn/>). The dataset stores over 244 million riding records between January and August 2021, which includes the user IDs and the coordinates and time information of OD. Notably, all user IDs are encrypted and no personal privacy information can be obtained (Table 1). In addition, considering the integrity and continuity of the raw dataset, we finally extract approximately 146 million records that occurred on all weekdays between April 8 and August 28, 2021 for the empirical study below (Fig.1). The exclusion of bike-sharing records during weekends and holidays is due to the substantial occurrence of non-commuting trips during these periods, which could increase data noise.

Moreover, this study acquired historical daily weather data for the study period (<https://lishi.tianqi.com/shenzhen/>) and public transportation station data (including location and passing bus or metro routes information) in 2021 (<https://lbs.amap.com/>). The former is

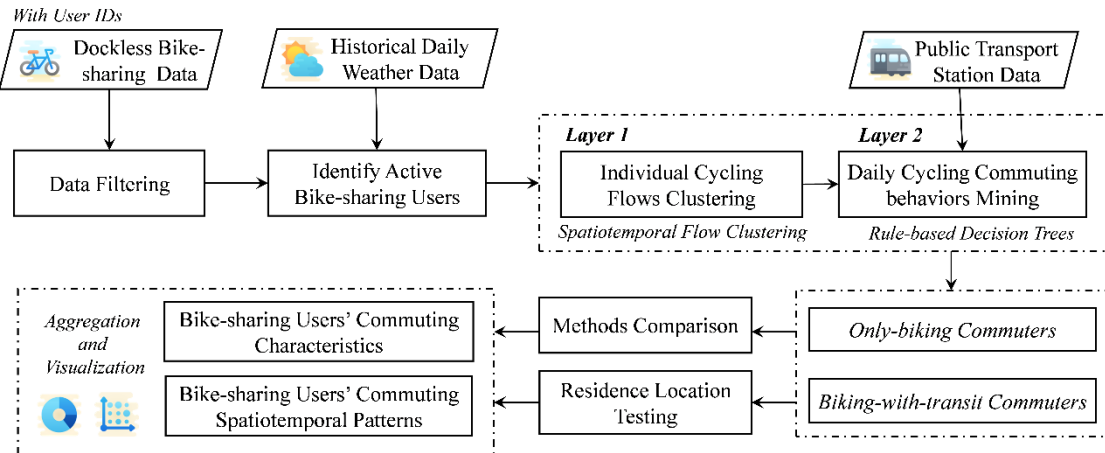
applied to extract active bike-sharing users, while the latter is employed to identify the transfer behaviors in individual daily commuting trips (details in Section 3).

Table 1 Example of dataset.

| User ID                 | Starting Time | Origin        | Ending Time | Destination   |
|-------------------------|---------------|---------------|-------------|---------------|
| 9fb2d1ec6142ace4d7405b  | 2021/01/30    | 114.0082,22.6 | 2021/01/30  | 114.0104,22.6 |
| *****                   | 13:19:32      | 392           | 13:23:18    | 348           |
| 1184eecf9f54441b389bcf* | 2021/01/31    | 113.8540,22.5 | 2021/01/31  | 113.8528,22.5 |
| *****                   | 23:49:12      | 884           | 23:54:37    | 840           |
| 30a457b24805ffab03b9c4  | 2021/01/30    | 114.0228,22.6 | 2021/01/30  | 114.0406,22.6 |
| *****                   | 13:09:10      | 506           | 13:23:24    | 404           |

### 3. Methodology

The flowchart of this paper depicted in Fig.2. Initially, "Data filtering and identify active bike-sharing users" step aims to eliminate abnormal cycling records and bike-sharing inactive users to enhance data quality. Then, the two-layer novel framework is employed to mine individual daily cycling commuting patterns, which is the centerpiece of this paper. Subsequently, "Evaluation and validation" step intends to examine the effectiveness and applicability of our framework through the comparative analyses of flow clustering methods and the testing of user's residences. Finally, we aggregate and visualize the mining results of bike-sharing users to reveal their commuting regularities and spatiotemporal patterns in the study area.



**Fig.2** Research flowchart of this paper.

### 3.1 Data filtering and identify active bike-sharing users

To ensure the accuracy and authenticity of the bike-sharing data applied to this study, anomalous or redundant records need to be cleaned. First, with reference to existing studies (Shen et al., 2018; Gao et al., 2021), the unrealistic long-or-short distances or durations cycling trips due to GPS drifting errors or user misoperations are eliminated. Afterwards, we aggregate the trips of each bike-sharing user based on user IDs and exclude duplicate records existing within the same user. Ultimately, about 2.53 million users' cycling records are extracted.

Moreover, by tallying the number of active days (i.e., have at least one trip record within a day) for users in the filtered weekdays data (Fig.3(a)), we also observe the issues of data sparsity. While some users heavily rely on bike-sharing for their daily activities, others, such as tourists or occasional cyclists, contribute sporadically to the dataset. For the latter, their limited trips cannot adequately capture their daily cycling habits. Hence, it is necessary to

exclude these sparse users to ensure a meaningful dataset for revealing relatively complete mobility patterns of individuals.

In a related study, Xu et al. (2018) defined active users in CDR data as those with at least one record for at least half of the study period. However, for bike-sharing dataset, it is crucial to consider the influence of weather on daily cycling. Existing studies have indicated that rainfall can significantly restrict cycling during commuting hours, as people tend to choose other safer transport modes (Reiss & Bogenberger, 2016; Shen et al., 2018). Similarly, in the dataset we used, bike-sharing usage is generally observed to be lower on drizzly and rainy days (Fig.3(b)). Hence, expanding on the approach of Xu et al. (2018), we exclude the rain-impacted weekdays to establish the threshold for active bike-sharing users, calculated as half of the total weekdays during the data collection period minus the number of drizzly and rainy days. In this study, with 100 weekdays and 21 drizzly and rainy days, the threshold is set at 29 days, thus identifying approximately 0.75 million active bike-sharing users for subsequent processing.

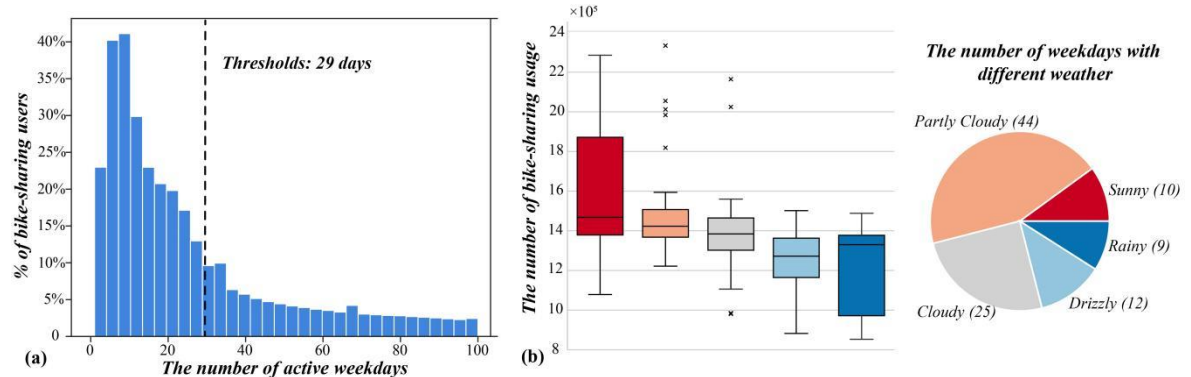
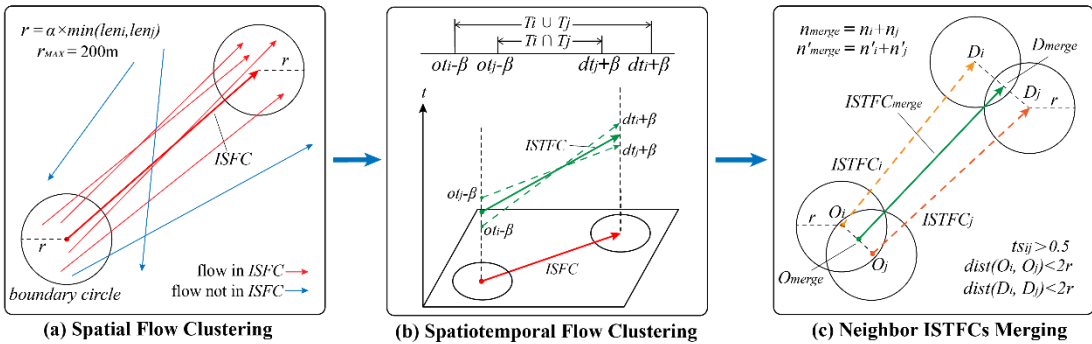


**Fig.3** (a) Histogram of the number of active days for bike-sharing users on weekdays; (b) Relationship between weekdays bike-sharing usage and different weather.

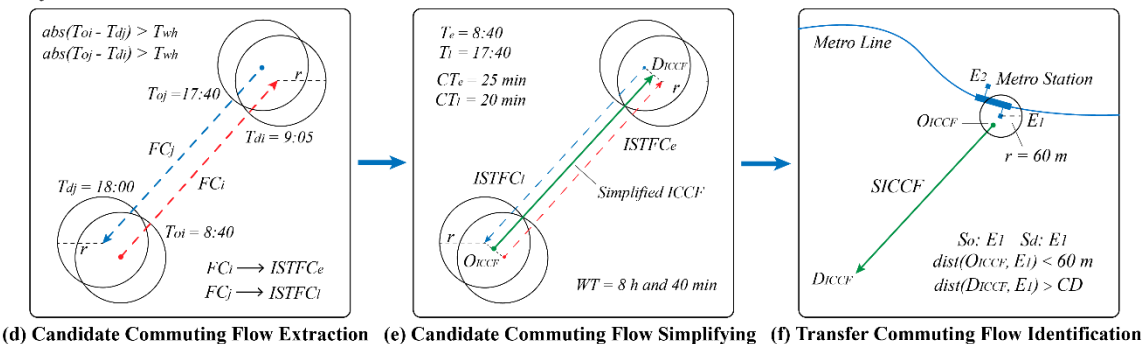
### 3.2 Two-layer framework for individual daily commuting patterns of bike-sharing users

Fig. 4 shows the diagram of our two-layer framework. In Layer 1, to address the lack of geocoding information for the OD of dockless bike-sharing records, we propose flow clustering methods with improved spatiotemporal constraints, tailored to the travel characteristics of bike-sharing, which can extract individual spatiotemporal flow clusters (ISTFCs) representing the user's daily cycling trajectories. In Layer 2, multiple rule-based decision trees that integrate round-trip journeys, working hours, and public transportation transfers is built to identify of bike-sharing commuting behaviors from the ISTFCs extracted in Layer 1.

#### Layer 1:



#### Layer 2:



**Fig.4** Schematic diagram of two-layer framework.

### 3.2.1 Layer 1: Individual cycling flows clustering

In this paper, the methods in Layer 1 can be divided into three essential steps: *Spatial flow clustering*, *Spatiotemporal flow clustering*, and *Neighbor ISTFCs merging*.

#### *Spatial flow clustering:*

This step aims to extract the daily trajectories of individual bike-sharing users from the spatial perspective. In this study, we apply the spatial flow clustering method proposed by Gao et al. (2020) and make enhancements based on the travel characteristics of bike-sharing. In the original method, spatial dissimilarity  $SD_{ij}$  is the key indicator for clustering, which is calculated as follows:

$$SD_{ij} = \sqrt{sd_{ijo}^2 + sd_{ijd}^2} \quad [1]$$

where  $sd_{ijo}$  and  $sd_{ijd}$  respectively represent the spatial dissimilarity between the OD of flows  $i$  and  $j$ , which are defined as follows:

$$\begin{cases} sd_{ijo} = \frac{dist(O_i, O_j)}{\alpha \times \min(len_i, len_j)}, \alpha \times \min(len_i, len_j) \leq 200 \\ sd_{ijd} = \frac{dist(D_i, D_j)}{\alpha \times \min(len_i, len_j)} \end{cases} \quad [2]$$

where  $dist(O_i, O_j)$  and  $dist(D_i, D_j)$  denote the Euclidean distance between the same endpoints of two flows.  $len_i$  and  $len_j$  are the lengths of two flows, respectively.  $\alpha$  is a size coefficient which sets the radius of the boundary circle together with  $\min(len_i, len_j)$ , as displayed in Fig.4(a). In this paper, referring to existing research (Gao et al., 2020, Liu et al., 2022),  $\alpha$  is set to 0.3.

However, note that the formula of  $SD_{ij}$  determines that the radius of the boundary circle

increases with the lengths of the flow, thereby reducing the spatial constraint on flow clustering. Although this feature has limited impact on regional-level flow studies, for individual-level related studies, it introduces the noise into clustering results and increases the uncertainty into the extent of individual's daily activities. For example, with  $\min(\text{len}_i, \text{len}_j) = 3000$  m, the boundary circle radius is 900 m, covering an area of  $2.54 \text{ km}^2$ . Hence, to obtain more realistic individual biking flows, we cap the maximum radius of boundary circle at 200 m, following precedents in bike-sharing research (Yang et al., 2019; Li et al., 2021). After settings parameters, flows  $i$  and  $j$  are deemed spatially similar if  $SD_{ij} \leq 1$  (Gao et al., 2020).

Then, taking all riding records of each active bike-sharing user as input, spatial flow clustering is performed according to the algorithm proposed by Gao et al. (2020). Finally, each individual spatial flow cluster (ISFC) can be denoted as  $\{ID_{USER}, ID_{ISFC}, (O, D), n\}$ , where  $ID_{ISFC}$  is the unique identifier of each ISFC,  $(O, D)$  are the OD medoids of all biking flows in ISFC, and  $n$  is the count of flows in ISFC. Notably, given that some ISFCs may include insufficient trips to represent a user's daily patterns, we set a minimum threshold for the number of biking flows in each user's ISFCs: one-fifth of the number of weekdays with recorded bike-sharing usage. Only the ISFCs that satisfy the threshold requirement are deemed reliable and advance to the next clustering step.

### ***Spatiotemporal flow clustering:***

Based on the results of the spatial flow clustering approach, this step further improves the spatiotemporal flow clustering method proposed by Yao et al. (2018) to extract individual user's daily mobility patterns from the temporal perspective. The core of their method is the

measurement of temporal similarity  $ts_{ij}$ , which is defined as follows:

$$ts_{ij} = \frac{T_i \cap T_j}{T_i \cup T_j} \quad [3]$$

where  $T_i = [ot_i, dt_i]$  and  $T_j = [ot_j, dt_j]$  denote the time spans of flows  $i$  and  $j$  in the same ISFC, respectively.  $T_i \cap T_j$  is their intersection, while  $T_i \cup T_j$  is their union (Fig.4(b)). If the time spans of  $i$  and  $j$  overlap,  $ts_{ij}$  is greater than zero. For instance, when  $T_i = [8:00, 8:40]$  and  $T_j = [8:15, 8:50]$ ,  $T_i \cap T_j$  is 25 min while  $T_i \cup T_j$  is 50 min, then  $ts_{ij}$  is 0.5.

It is noteworthy that, due to the individual-level focus and the average of 3.6 bike-sharing trips per weekday among active users, our study deems it is impractical to calculate  $ts_{ij}$  for travel flows on specific adjacent dates, as conducted by Yao et al (2018). Instead, this paper concentrates on the temporal distribution of cycling activities within a 24-hour timeframe. Simultaneously, this strategy is also more conducive to capturing the genuine mobility of bike-sharing users, because most residents follow regular daily travel patterns, especially commuting trips. For instance, suppose that  $T_i$  above occurs on Monday and  $T_j$  on Friday, we still assume that their time spans overlap. Moreover, previous research has validated the application of the temporal similarity indicator in taxi trip data (Yao et al., 2018). Nevertheless, bike-sharing trips are typically shorter (the average cycling duration for the dataset we used is around 10 min), which can result in a zero temporal similarity even if the travel times of the two biking flows are sufficiently close (e.g., when  $T_i=[8:05,8:15]$  and  $T_j=[8:15,8:25]$  ,  $ts_{ij}=0$ ). To address this, we introduce an expansion coefficient  $\beta$  to  $T_i$  and  $T_j$  (i.e.,  $T_i = [ot_i - \beta, dt_i + \beta]$  and  $T_j = [ot_j - \beta, dt_j + \beta]$ ) to ensure that the time-adjacent cycling flows can be identified and clustered. In this study,  $\beta$  is set to 30 min (more details

in Section 4.1). After the above improvement, referring to the original method, we consider that the travel times of flows  $i$  and  $j$  are adjacent when  $ts_{ij} \geq 0.5$ .

Later, we use the biking records including in each user's ISTC as input and execute the spatiotemporal flow clustering algorithm by Yao et al. (2018). Ultimately, each ISTFC can be denoted as  $\{ID_{USER}, ID_{ISFC}, ID_{ISTFC}, (O, D), n', T_o, T_d\}$ , where  $ID_{ISFC}$  is the unique identifier of the ISFC to which the ISTFC belongs,  $ID_{ISTFC}$  is the unique identifier of each ISTFC.  $n'$  is the number of biking flows in the ISTFC, and  $T_o$  and  $T_d$  are the average starting and ending time of these flows, respectively. The resulting ISTFCs are used in the subsequent processing.

#### ***Neighbor ISTFCs merging:***

By observing the result of spatiotemporal flow clustering, we find that some ISTFCs are spatiotemporally adjacent but not merged, as illustrated in Fig.4(c). The reasons are relevant to two aspects: First, some bike-sharing users have multiple optional routes to and from the same daily activity places. The locations of ODs (e.g., different entrances to an industrial park) and the direction of their trip flows vary with the different routes, which leads to difficulties in clustering them into the same ISTFC. Second, in "*Spatial flow clustering*" step, the restriction of boundary circle may result in dividing the cycling flows into more ISFCs. Nevertheless, the improvement of  $SD_{ij}$  is essential to extract more accurate trajectories of individual daily activities. To improve the utilization of biking records for these affected users, we examine and merge neighboring ISTFCs in the last step of Layer 1.

Given a set of all ISTFCs for an active bike-sharing user  $FC$  and the size coefficient  $\alpha$ , the process of neighbor ISTFCs merging is shown in Algorithm 1. In short, two ISTFCs  $FC_i$

and  $FC_j$  that can be merged must satisfy the following conditions:

- (1) The temporal similarity  $ts_{ij}$  is not less than 0.5, which is consistent with "***Spatiotemporal flow clustering***" step;
- (2) The boundary circle at the same endpoints of  $FC_i$  and  $FC_j$  must intersect (i.e., the distance between these endpoints should be less than twice of  $\alpha \times \min(len_i, len_j)$ ), and the radius of the boundary circle is calculated consistent with "***Spatial flow clustering***" step.

When  $FC_i$  and  $FC_j$  satisfy the above conditions,  $FC_j$  is merged by  $FC_i$ . Meanwhile, the attributes of  $FC_i$  are also to  $FC_{merge}$  in Fig. 4(c).

---

**Algorithm 1** Merging Neighbor ISTFCs

---

**Input:**  $FC = \{FC_i | 1 \leq i \leq n\} \leftarrow$  a set of all ISTFCs for an active bike-sharing user; and  $\alpha$   
 $\leftarrow$  the size coefficient;

**Steps:** **For each** ISTFC  $FC_i$ , where  $1 \leq i \leq n$

**For each** ISTFC  $FC_j$ , where  $i < j \leq n$

**If**  $\alpha \times \min(len_i, len_j) > 200$  **then**

$\alpha \times \min(len_i, len_j) = 200$

**If**  $ts_{ij} \geq 0.5$  and  $dist(O_i, O_j) < 2\alpha \times \min(len_i, len_j)$  **then**

and  $dist(D_i, D_j) < 2\alpha \times \min(len_i, len_j)$  **then**

Merge the two ISTFCs:  $FC_i \leftarrow FC_i \cup FC_j$  and  $FC \leftarrow FC / FC_j$

**Return:** A set of all ISTFCs for this user after merging  $FC = \{FC_i | 1 \leq i \leq m\}$ .

---

Similarly, through the above flow clusters merging process, some ISTFCs still have

limitations in representing the mobility of individual activity due to the small number of trips they contain. To do so, we set a minimum threshold for filtering ISTFCs: an ISTFC must contain at least 20% of the number of biking flows within its corresponding ISFC (i.e.,  $n' \geq 0.2 \times n$ ). Only the ISTFCs that satisfy this threshold are deemed reliable and employed as inputs to Layer 2.

### 3.2.2 Layer 2: Daily cycling commuting behaviors mining

While the ISTFCs acquired in Layer 1 capture the spatiotemporal patterns of individual daily mobility, they lack semantic information about the associated activities. In Layer 2, we build three rule-based decision trees considering round-trip journeys, working hours, and public transportation transfers, aiming to mine individual commuting patterns from the ISTFCs of bike-sharing users.

Initially, we develop the "*Candidate commuting flow identifier*" decision tree (Fig.5), focusing on round-trip frequencies and working hours. This identifier aims to extract latent daily commuting patterns, i.e., individual candidate commuting flows (ICCFs), from the ISTFCs of bike-sharing users. Specifically, we define an ICCF by below two criteria:

- (1) The commuting behavior should be characterized by frequent and symmetrical (i.e., round-journeys) travel flows between two locations (Liu et al., 2023);
- (2) There should be a substantial time interval between the biking flows in opposite directions, symbolizing the user's daily working hours.

Hence, in "*Candidate commuting flow identifier*", given two ISTFCs  $FC_i$  and  $FC_j$  for a bike-sharing user, we firstly assess spatial adjacency of their opposite endpoints. Specifically, we require that both  $dist(O_i, D_j)$  and  $dist(O_j, D_i)$  be less than boundary circle

radius  $r$ . The calculation of  $r$  is consistent with Layer 1. If  $FC_i$  and  $FC_j$  meet the spatial adjacency, we further evaluate whether the time interval between them exceeds the minimum working hours threshold  $T_{wh}$ , as shown in Fig.4(d). Following Sari Aslam et al. (2019), this paper establish  $T_{wh}$  at 4 hours to effectively capturing the daily working behaviors of full-time, part-time, and shift workers. If  $FC_i$  and  $FC_j$  satisfy the above two conditions, they are marked as an ICCF for follow-up analysis. Each ICCF can represented as  $\{ID_{USER}, ID_{ICCF}, ISTFC_e, ISTFC_l\}$ , where  $ISTFC_e$  and  $ISTFC_l$  denote the ISTFCs with earlier and later travel time, respectively. Notably, before inputting the user's ISTFCs into the identifier, we sort them by the number of cycling flows they encompass in descending order. This step is taken because larger flow clusters tend to encapsulate user's daily activity patterns. Meanwhile, by prioritizing the traversal of these clusters, we also can expedite the ICCF extraction process.

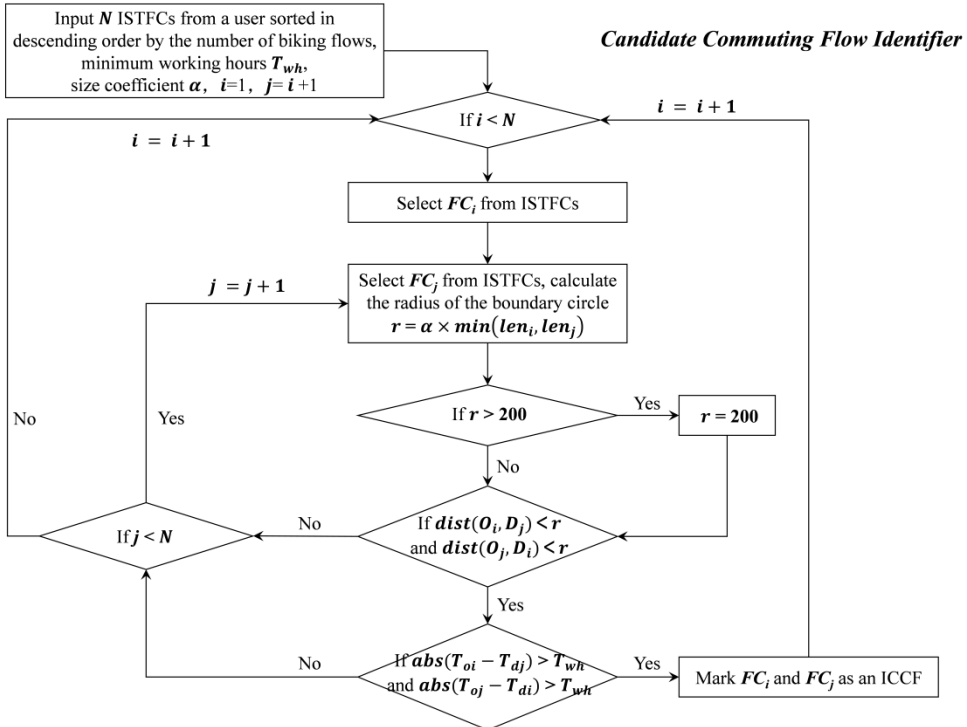


**Fig.5** Flowchart of candidate commuting flow identifier.

Afterwards, to facilitate subsequent analysis, we simplify the identified ICCF consisting of a pair of ISTFCs into a single flow (Fig.4(e)). The direction of simplified ICCF (SICCF) is set to match the ISTFC with earlier travel time (i.e.,  $ISTFC_e$ ). Thus, for each SICCF, its origin (i.e.,  $O_{ICCF}$ ) is the midpoint of the origin of  $ISTFC_e$  and the destination of  $ISTFC_l$ . Conversely,  $D_{ICCF}$  is the midpoint of the origin of  $ISTFC_l$  and the destination of  $ISTFC_e$ . Additionally, we define the following eight attributes for each SICCF to identify and analyze individual daily commuting patterns:

- (1) Departure time for the ISTFC with earlier travel time ( $T_e$ ): the  $T_o$  of  $ISTFC_e$ ;
- (2) Departure time for the ISTFC with later travel time ( $T_l$ ): the  $T_o$  of  $ISTFC_l$ ;
- (3) Cycling time for the ISTFC with earlier travel time ( $CT_e$ ): the difference between  $T_o$  and  $T_d$  of  $ISTFC_e$ ;
- (4) Cycling time for the ISTFC with later travel time ( $CT_l$ ): the difference between  $T_o$  and  $T_d$  of  $ISTFC_l$ ;
- (5) Cycling commuting distance ( $CD$ ): the Euclidean distance between  $O_{ICCF}$  and  $D_{ICCF}$ ;
- (6) Working hours ( $WH$ ): the difference between the  $T_d$  of  $ISTFC_e$  and the  $T_o$  of  $ISTFC_l$ ;
- (7) Total number of biking flows ( $n_t$ ): the sum of the biking flows in  $ISTFC_e$  and  $ISTFC_l$ ;
- (8) Cycling round-trip rate ( $R_{rt}$ ): the ratio of the number of biking flows in  $ISTFC_l$  and  $n_t$ , this indicator can measure the imbalance in commuting frequencies between the two opposite directions

Each SICCF is represented as

$$\{ID_{USER}, ID_{ICCF}, (O_{ICCF}, D_{ICCF}), T_e, T_l, CT_e, CT_l, CD, WH, n_t, R_{rt}\}.$$

Next, we establish the "**Transfer commuting flow identifier**" decision tree (Fig.6), accounting for public transit transfers, to identify latent daily transfer commuting behaviors from users' SICCFs. This consideration arises from research indicating that transferring to public transportation, especially the metro, is the important travel purpose of bike-sharing (Xing et al., 2020; Li et al., 2021). Additionally, the integrated use of bike-sharing and public transportation has attracted significant research attention recently (Ma et al., 2019; Guo & He, 2020; Kim, 2023). Therefore, it is crucial to determine whether bike-sharing users regularly cycle to connect with public transit for their daily commuting. The workflow of the identifier in Fig. 6 is described as follows:

- (1) Take the public transport station data and a user's SICCF as input, and set a maximum transfer distance threshold  $TD$ . In this study, the  $TD$  is set to 60 m for metros referring to Liu et al. (2022), and 30 m for buses, which are deemed less attractive for bike-sharing (Guo & He., 2020)
- (2) If the SICCF's departure time is outside the public transportation operating hours (from 6:00 to 23:30 in our study area), it is considered not connected to public transport. Conversely, we continue.
- (3) Identify the nearest public transport stations to the OD of the SICCF (i.e.,  $O_{ICCF}$  and  $D_{ICCF}$ ), labeled as  $S_o$  and  $S_d$ , respectively. If  $dist(O_{ICCF}, S_o)$  and  $dist(D_{ICCF}, S_d)$  both exceed  $TD$ , this SICCF is deemed to not connected to public transit. Conversely, we proceed.
- (4) If  $dist(O_{ICCF}, S_o) < dist(D_{ICCF}, S_d)$ , i.e., the SICCF's origin is closer to its nearest public transport station, we still cannot conclude that this user regularly commutes

to and from the work by bike-sharing from the transfer station. This is because public transport stations often coexist with various activity places, especially around metro stations (Liu et al., 2022). In this case, we need further compare the distance from the SICCF's other endpoints (i.e.,  $D_{ICCF}$ ) to its nearest public transport station (i.e.,  $S_d$ ) with this SICCF's length (i.e.,  $CD$ ). If  $dist(D_{ICCF}, S_d) < CD$  and  $S_o$  and  $S_d$  are on the same public transit line, it is argued that the SICCF is not connected to public transit, because as the user has chosen a longer cycling route instead of a shorter public transport journey (see Fig.A.1 in Appendix A in Supplemental files). Conversely, it is inferred that this SICCF's origin is connected to public transportation (see Fig.4(f)). Similarly, if  $dist(O_{ICCF}, S_o) \geq dist(D_{ICCF}, S_d)$

Note that for each SICCF, we employ the "***Transfer commuting flow identifier***" to assess connections with bus and the metro systems. When a SICCF qualifies for connectivity with both, the metro is prioritized over the bus (Guo & He., 2020).

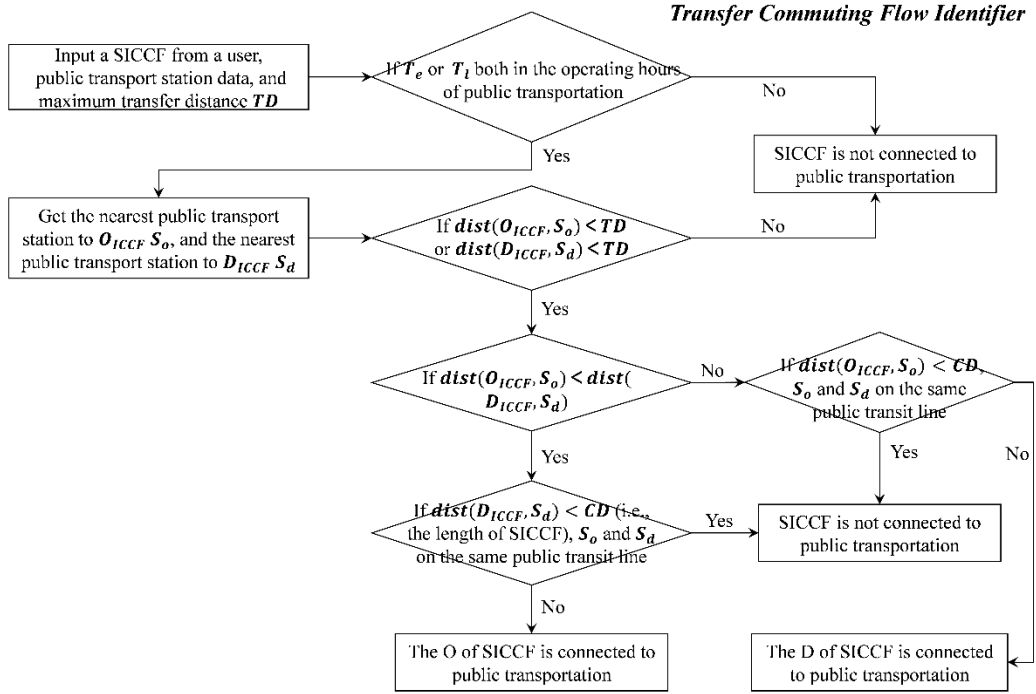


**Fig.6** Flowchart of transfer commuting flow identifier.

Finally, we build the "***Biking commuting user classifier***" decision tree to identify and categorize the most predominant daily commuting patterns among individual bike-sharing users (Fig.7). In our study, the SICCF with the highest count of biking records (i.e.,  $n_t$ ) is deemed most representative of a bike-sharing user's daily commuting patterns during the study period and is designated as the individual daily commuting flow (IDCF). Users are classified into two main categories: *Only-biking* and *Biking-with-transit commuters*, and the latter is further subcategorized into: *Biking-transit*, *Transit-biking*, and *Biking-transit-biking commuters*, drawing insights from relevant studies (Singleton & Clifton, 2014; Guo et al., 2021). The definition of the different user categories in Fig.7 are outlined as follows:

- (1) Take the IDCF for a user as the input.
- (2) If the IDCF lacks a connection to public transit, this user is classified as an *Only-biking* user.

*biking commuter* who relies solely on biking for his/her daily home-work commuting.

The OD of the IDCF represent this user's residence and workplace, respectively.

Conversely, it proceeds to the next step.

(3) If the IDCF's origin is connected to public transit, it signifies that the IDCF represents the user's daily "last-mile" commuting to work by bicycling from a transit station (or the "first-mile" commuting from his/her workplace to the transit station after work). The IDCF's origin indicates the transit station where the user starts daily his/her cycling to work, while the destination stands for his/her workplace. However, in this scenario, the user's daily commuting process is incomplete, as it lacks the segment where the user travels between the residence and another transfer station. Thus, we need search for his/her remaining SICCFs that satisfy the following conditions to form his/her complete daily commuting chain:

- The of this SICCF destination is connected to public transportation;
- The transfer station of this SICCF and the IDCF are different;
- This SICCF is temporal close to the IDCF, meaning the time difference between this SICCF's and the IDCF's  $T_e$  and the time difference between this SICCF's and the IDCF's  $T_l$  are both less than 1 hour.

If an SICCF meeting the above conditions is found, it is labeled as an individual additional daily commuting flow (IADCF), and the process proceeds to the next step.

Otherwise, the user is considered a *Transit-biking commuter*, who relies solely on biking for the "last mile" from transit station to his/her workplace (or the "first mile" from his/her workplace to transit station after work). Similarly, if the IDCF's origin

is connected to public transit but no suitable IADCF is identified among the user's remaining SICCFs, the user is categorized as a *Biking-transit commuter*, who relies exclusively on bicycling for the "first mile" from his/her residence to transit station (or the "last mile" from transit station to his/her residence after work).

(4) If the origin of the user's IDCF is connected to a transit station and an IADCF is identified, this IADCF represents the user's daily "first mile" commuting by bicycling from his/her residence to another transit station (or the "last mile" commuting when returning home from another transfer station after work). In this scenario, by combining the IDCF with the IADCF, the complete daily commuting pattern, including residential and workplace locations, can be established. Meanwhile, this user is categorized as a *Biking-transit-biking commuter* (See Fig.A.2 in Appendix A in Supplemental files for an illustration). Likewise, if the destination of a user's IDCF is connected to public transit while an IADCF is found, this user is also classified a *Biking-transit-biking commuter*.

In Fig.8(a), we illustrate a schematic categorizing the aforementioned bike-sharing commuters. Moreover, there are differences in the commuting characteristics of the various categories of bike-sharing commuters. For further details, refer to Appendix B in Supplemental files.

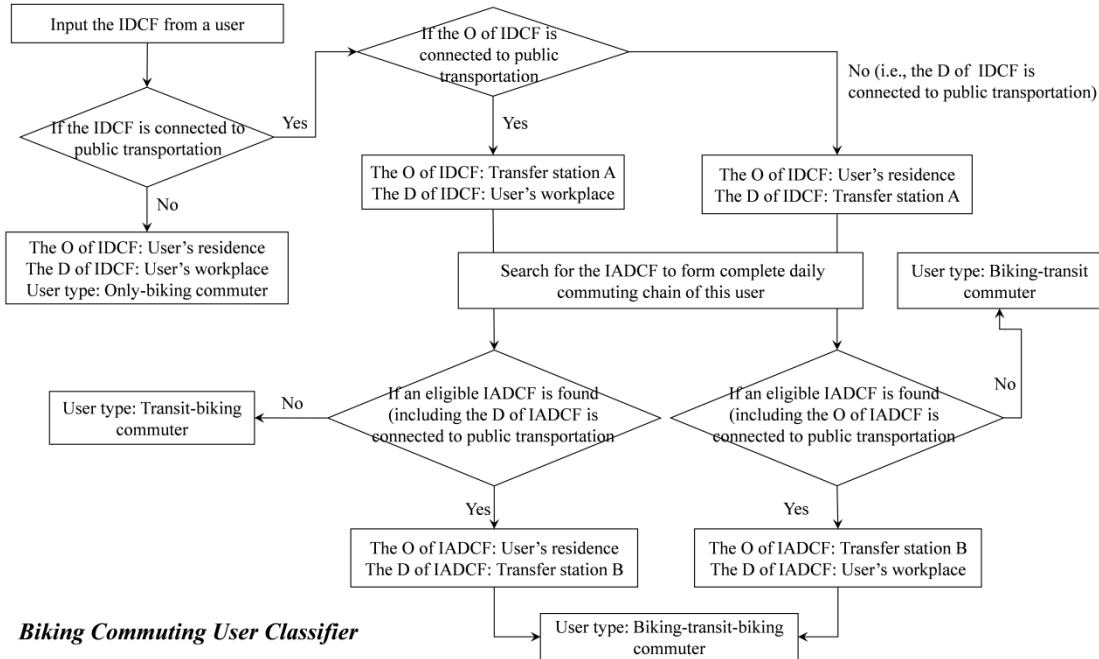


**Fig.7** Flowchart of biking commuting user classifier.

### 3.3 Evaluation and validation

To demonstrate the feasibility and applicability of our proposed two-layer framework, this paper will evaluate the performance of the improved spatiotemporal flow clustering methods and validate the identification results of residential locations of bike-sharing commuters.

For Layer 1, we contrast the clustering results of the original methods with our enhanced methods using multiple indicators. For *spatial flow clustering* method, we computed four indicators: the average number of biking records included in each ISFC, the average length of ISFCs, and the average distance from the OD of each biking record to the OD of its corresponding ISFC (later abbreviated as the average distances to ISFCs' origins and destinations, respectively). These indicators are used to highlight the promoting of restricting

the boundary circle radius for more precise daily cycling trajectories extraction. For ***spatiotemporal flow clustering*** method, we examine the impact of different expansion coefficients  $\beta$  on the average number of biking records contained in each ISTFC and the average maximum time interval within each ISTFC (i.e., the mean difference between the earliest departure and the latest arrival times of the trip records within each ISTFC). This analysis is aimed at illustrating the necessity of expansion coefficient in mining spatiotemporal mobility for bike-sharing trips.

For Layer 2, due to the unavailability of travel survey data on cycling habits within the study area and the significant bias between the census population and the bike-sharing users, this work decides to employ residential land use data (Accessed from Shenzhen Municipal Housing and Construction Bureau, <https://zjj.sz.gov.cn/fwzljgcx>) to validate the accuracy of our extracted users' residences. Specifically, we first extract the users who have identifiable residential locations, then measured the distances from their residence to the actual boundaries of residential land parcels. If a user's residence falls in the residential land, the distance is set to zero. Lastly, we plot the cumulative percentage of users whose identified residences are within 0 to 300 meters of the actual residential land. If the majority of users' residence are located within or near the actual boundaries of residential land, it would demonstrate a close match between the bike-sharing commuters' residences and the actual residential land use distribution. Notably, this paper does not perform the same validation for users' workplace identified, as residents in occupations have diverse workplace not limited to office spaces or industrial parks, which is more likely to lead to omissions and misclassifications.

### 3.4 Aggregation and visualization analysis

Based on the identification and validation results of bike-sharing commuters, we further aggregate and analyze their daily commuting characteristics (i.e., commuting duration and distance, working hours, and cycling round-trips rate) and spatiotemporal patterns (i.e., commuting temporal patterns, spatial distribution of residences, workplaces, metro transfer stations, and commuting chains) within the study area.

## 4 Result and discussions

### 4.1 Methods evaluation and validation results

In Table 2, we compare the evaluation indicators between the original and improved ***spatial flow clustering*** methods. Obviously, compared to the enhanced method, the original method exhibits a slight increase in the average number of trip records within each ISFC (an average increase of 3 additional biking records) due to the absence of the boundary circle constraints. Meanwhile, notable changes are observed in the average distances to ISFC's OD, with increases of 23 m and 16 m, respectively.

Recognizing the significant impact of the boundary circle radius constraint on longer ISFCs, we conducted additional comparison for ISFCs exceeding lengths of 1500 m and 3000 m. The results reveal that while the average distances to the ISFC's OD maintains nearly constant with increasing ISFC length in the enhanced method, they rise substantially in the original method. However, the magnification of these two indicators implies significant uncertainty in determining the OD of longer ISFCs, as their boundary circles have excessively broad coverage. These uncertainties may introduce more inaccuracies in

subsequent analyses (e.g., identifying users' residences and workplaces). Consequently, the enhancement of *spatial flow clustering* introduced in this study are essential, ultimately extracting reliable ISFCs from 95.1% (~0.71 million) of active bike-sharing users.

**Table 2** Comparison of evaluation indicators between the original and improved *spatial flow clustering* methods (see Section 3.3 for descriptions of below indicators).

| Method   | Original method | Improved method |
|--|-----------------|-----------------|
| <b>Avg. number of biking records</b>                     | 43.5 (26.7)     | 40.7 (25.3)     |
| <b>Avg. distance to ISFC's origin (unit: m)</b>          | 105 (111)       | 82 (64)         |
| <b>Avg. distance to ISFC's destination (unit: m)</b>     | 80 (89)         | 64 (51)         |
| <b>Pct. of ISFCs more than 1500 m</b>                    | 24.40%          | 23.06%          |
| <b>Avg. distance to ISFC's origin (&gt; 1500 m)</b>      | 162 (161)       | 83 (63)         |
| <b>Avg. distance to ISFC's destination (&gt; 1500 m)</b> | 118 (138)       | 63 (50)         |
| <b>Pct. of ISFCs more than 3000 m</b>                    | 4.69%           | 4.21%           |
| <b>Avg. distance to ISFC's origin (&gt; 3000 m)</b>      | 214 (232)       | 84 (64)         |
| <b>Avg. distance to ISFC's destination (&gt; 3000 m)</b> | 156 (215)       | 61 (49)         |

\* The values in bracket are standard deviations of the corresponding indicators.

Similarly, Table 3 displays the comparative results of the original and enhanced *spatiotemporal flow clustering* methods. Clearly, in contrast to the original method ( $\beta=0$ ), the improved method, incorporating an expansion coefficient  $\beta$ , can extract ISTFCs that contain more trip records (averaging an increase of 7.1 records including in each ISTFC when  $\beta=30$  min). This substantiates the promoting effect of the  $\beta$  in mining daily spatiotemporal trajectories from bike-sharing data, given the generally shorter travel durations for bicycle trips. However, as  $\beta$  increases further, the average number of trip records within ISTFCs

shows diminishing returns, with an increase of only 0.9 records at  $\beta=90$  min compared to  $\beta=60$  min. Meanwhile, the average maximum time interval for each ITSFC continues to increase with the growing of  $\beta$ . Yet, an excessively large average maximum time interval could introduce biking records from other time periods into the extracted ISTFCs, potentially elevating data noise. Hence, this study refers to the China Urban Transportation Report 2021 (<https://jiaotong.baidu.com/cms/reports/traffic/2021/index.html>) and select a final  $\beta$  value of 30 min, which is remarkably close to the average commuting duration in Shenzhen (37 min). Ultimately, through the processes of ***Spatiotemporal flow clustering*** and ***Neighbor ISTFC merging***, we successfully identify reliable ISTFCs from 74.4% (~0.56 million) of active bike-sharing users. Notably, ~0.11 million reliable ISTFCs from over 90,000 users are accomplished through ***Neighbor ISTFC merging*** step. Collectively, these results underscore the critical role of the aforementioned enhancements in Layer 1 in improving the quality of daily travel trajectories extraction for bike-sharing users.

**Table 3** Comparison of evaluation indicators between the original and improved ***spatiotemporal flow clustering*** methods (see Section 3.3 for descriptions of below indicators)

| Method  | Original method | Improved method      |                      |                      |
|---|-----------------|----------------------|----------------------|----------------------|
|   | $\beta=0$       | $\beta=30\text{min}$ | $\beta=60\text{min}$ | $\beta=90\text{min}$ |
| <b>Avg. number of biking records</b>                        | 12.5 (10.3)     | 19.6 (14.8)          | 21.3 (15.3)          | 22.4 (15.6)          |
| <b>Avg. maximum time interval of each ITSFC (unit: min)</b> | 16.8 (11.7)     | 34.8 (13.9)          | 49.1 (20.3)          | 61.8 (27.0)          |

\* The values in bracket are standard deviations of the corresponding indicators.

Furthermore, utilizing the rule-base decision trees from Layer 2, we have successfully

extracted the IDCFS of 383,786 active bike-sharing users with reliable ISTFCs. Fig.8(b) illustrates the proportion of identified bike-sharing commuters in different categories: 74.38% are *Only-biking commuters* and 25.62% are *Biking-with-transit commuters*. The percentage of *Biking-with-transit commuters* is slightly higher than the results for transfer trips in the studies of Xing et al. (2019) and Li et al. (2020) regarding the purpose of bike-sharing trips, while they considered more kinds of travel activities. Within these *Biking-with-transit commuters*, the share of *Biking-transit-biking commuters* is only 1.75% due to the stringent filtering rules, while *Biking-transit commuters* (14.39%) are more prevalent than *Transit-biking commuters* (9.48%), aligning with the findings of Guo et al. (2020), which suggests that more users rely on cycling for the "first mile" from residence to transit station (or the "last mile" from transit station to home after work). Meanwhile, given that the majority of bike-sharing commuters daily transfer to the metros (over 96%) rather than the buses, our subsequent analysis will focus on the integrated biking-metro commuting patterns.

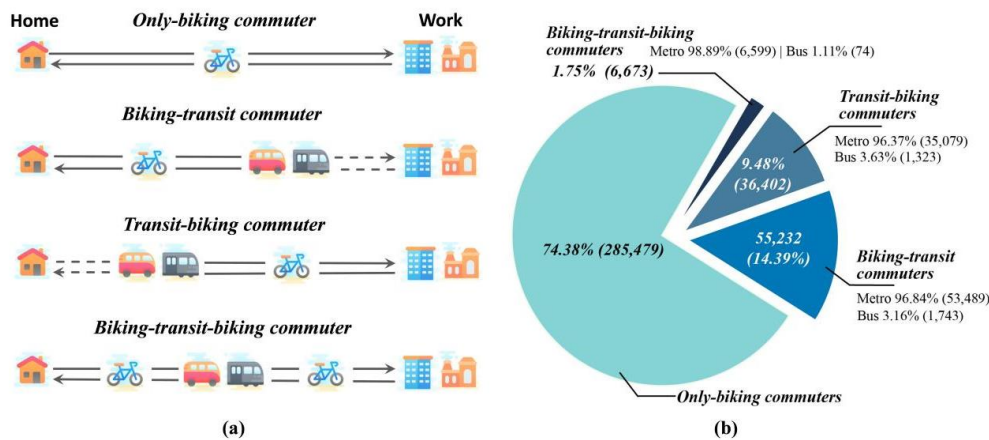


**Fig.8** Schematic diagram (a) and percentage (b) of different categories of bike-sharing commuters.

To further validate the accuracy of the identification results of bike-sharing commuters, a comparison is made between the distribution of their identified residences and the actual residential land use boundaries (see Section 3.3 for details), as showed in Fig.9. The result illustrates that 51.5% of inferred users' residences are within the residential land are, and 93.5% are within 100 m of the residential land use. These findings indicate that the most of the identified users' homes are within or adjacent to the actual residential land parcels, reflecting the feasibility and effectiveness of our two-layer framework.

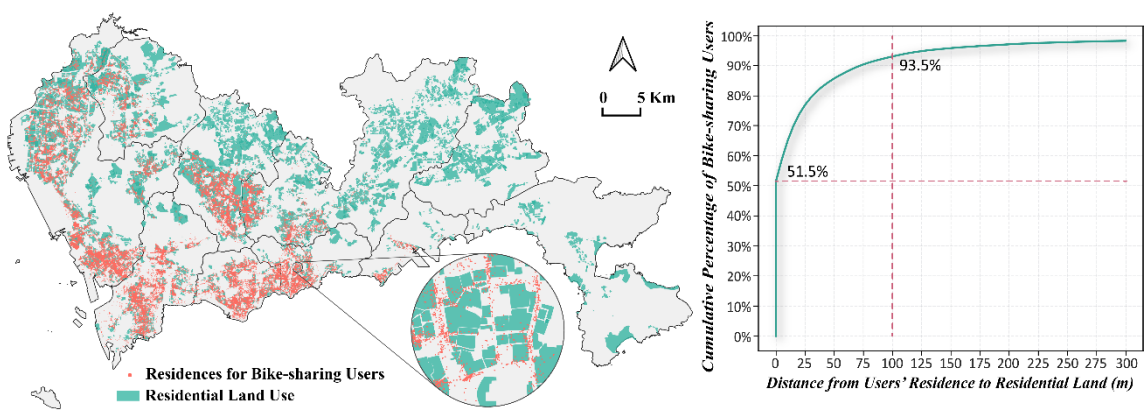


**Fig 9.** Cumulative percentage of bike-sharing users whose identified residences fall within the residential land boundaries.

#### 4.2 Commuting characteristics among bike-sharing users

##### 4.2.1 Commuting duration and distance

Fig.10 shows the distribution of commuting duration and distance for *Only-biking* and *Biking-transit-biking* commuters. Since the commuting chains for *Transit-biking* or *Biking-transit* commuters are incomplete, we cannot discuss these commuting characteristics for them. For *Only-biking* commuters (Fig.10(a, b)), we find that over three-quarters have a daily commuting duration under 10 min and distance within 1.8 km, aligning with previous

research (Shen et al., 2018; Ma et al., 2020; Gao et al., 2022), which suggests that most *Only-biking commuters* are more likely to reside near their workplaces. For *Biking-transit-biking commuters* (Fig.10(c, d)), we observe an average commuting duration exceeding 45 min and distance over 13 km, indicating that these users tend towards complete their daily home-work commuting across districts. Moreover, when comparing the commuting duration distribution for different trip purposes (Fig.10(a, c)), we notice that both bike-sharing commuting groups tend to spend more time commuting home from work, consistent with the results of Kung et al. (2014), which can be attributed to having more intervening opportunities for other activities (e.g., recreation, shopping and etc.) during their journey home.

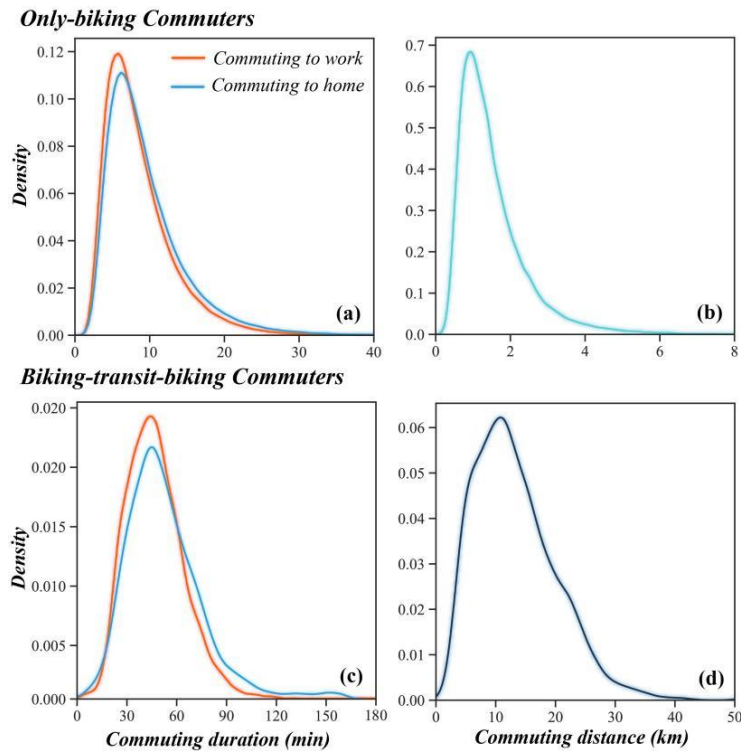


**Fig. 10** Distributions of commuting duration (a, c) and commuting distance (b, d) for *Only-biking* and *biking-transit-biking* commuters

#### 4.2.1 Working hours

Fig.11(a) displays the working hours distribution for all bike-sharing commuters, excluding *Biking-transit commuters*, for whom we only obtain the commuting chains between their residence and transfer station. Specially, we identify three distinct peaks for *Only-biking commuters*' working hours. The largest peak occurs at 10 hours, which is longer than the common sense of eight-hour work schedule. However, note that the working hours we calculated are the total time from user's daily arrival to departure at the workplace, potentially including non-working hours like lunch breaks. Thus, the actual working hours for many individuals are likely 1 to 2 hours less than the working hours we calculated. This indicates that the working hours for most users are in accordance with legal regulations. The second highest peak, observed at approximately 12.5 hours, implies that some users are actually working overtime, even if their calculated working hours include breaks. Lastly, the smallest peak, appearing at around 5 hours, which is significantly lower than the first two peaks and represents a minority of individuals working part-time or on shift.

In contrast to *Only-biking commuters*, *Biking-transit* and *Biking-transit-biking commuters* exhibit a single prominent peak in their working hours, which is consistent with the largest peak for *Only-biking commuters*. Furthermore, while some *Biking-with-transit commuters* also work overtime, as indicated by a slight peak after 12 hours, the proportion is far less than *Only-biking commuters*. This reflects that *Only-biking commuters* are more tolerant of overtime than *Biking-with-transit commuters*, one reason for which may be their lower commuting costs. Lastly, we discover that bike-sharing users who involved in part-time or shift work rarely connect to public transportation for commuting. That is reasonable, as they work around 5 hours and choosing a biking-with-transit commuting mode represents

excessively high proportion of their commuting duration relative to working hours (Schwanen & Dijst, 2002).

#### 4.3.3 Cycling round-trip rate

Cycling round-trip rate is an indicator that measures the regularity differences between commuting to and from work by bike. Generally, as shown in Fig.11(b), there is little difference in the cycling round-trip rates among various kinds of commuters (due to the small number of *Biking-transit-biking commuters*, their distribution is more concentrated). The average cycling round-trip rate is around 0.6, with the lower quartile roughly 0.5, indicating that for nearly three-quarters of bike-sharing commuters, riding to work is more regular than riding home. In other words, the behavior of cycling to work is more likely to be observed for most users. That could be that residents have fewer time constraints and more autonomous activities after work. Additionally, it could also be due to the insufficient supply of bike-sharing, which leads some users to choose alternatives for the return journey.

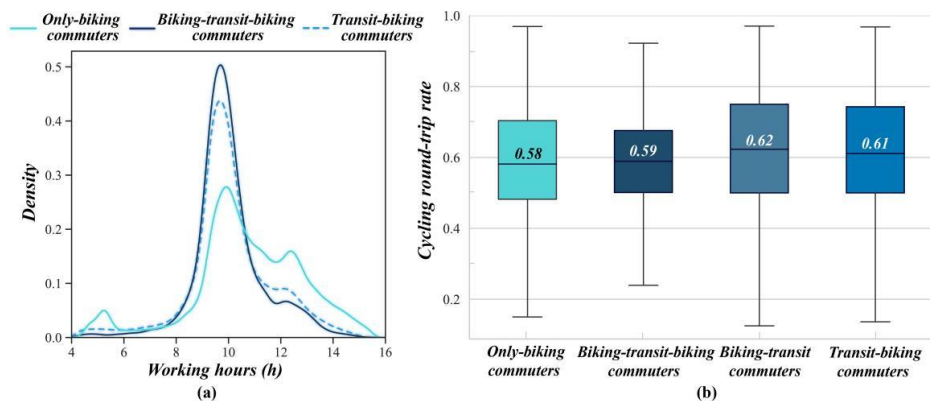


**Fig. 11** (a) Distribution of working hours for *Only-biking*, *Transit-biking* and *Biking-transit-biking* commuters; (b) Distribution of cycling round-trip rate for different kinds of bike-sharing commuters.

## 4.3 Commuting spatiotemporal patterns among bike-sharing users

### 4.3.1 Temporal patterns of bike-sharing commuters

In Fig.12, we present the daily commuting temporal patterns for different kinds of bike-sharing commuters. However, due to the incomplete commuting chains of *Transit-biking commuters*, as mentioned earlier, we cannot discuss their home-to-work temporal patterns. Similarly, we omit the work-back-home temporal patterns for *Biking-transit commuters*.

Concerning the temporal patterns of commuting to work (Fig.12(a)), we observe that the sharp peak for *Biking-transit* and *Biking-transit-biking commuters* both occur before 8:00, while the peak for *Only-biking commuters* is around 8:30. This result combined with the observation in Fig.10 suggests that users with higher commuting costs tend to depart earlier, consistent with Kung et al. (2014). Moreover, the departure time of *Biking-transit commuters* is slightly later than that of *Biking-transit-biking commuters*, indicating that their commuting durations are shorter overall and their workplaces are closer to transfer stations.

Regarding the temporal patterns of commuting back home (Fig.12(b)), we find that the peak of all three kinds of commuters appear around 18:30, which reflects the standard off-duty commuting time for most bike-sharing users. However, this also means a massive demand for bike-sharing during the same period, especially around the workplaces. If bicycles supply is insufficient, some users have to choose alternative transportation modes, which explains why the cycling round-trip rate for most users are more than 0.5 (Fig.11(b)). Furthermore, compared to commuting to work, the smoother curve and extended tail (20:00-23:00) for commuting back home once again reflects the phenomenon of some users working overtime, with a high proportion of *Only-biking commuters*, which echoes the discussion in

Fig.11(a).

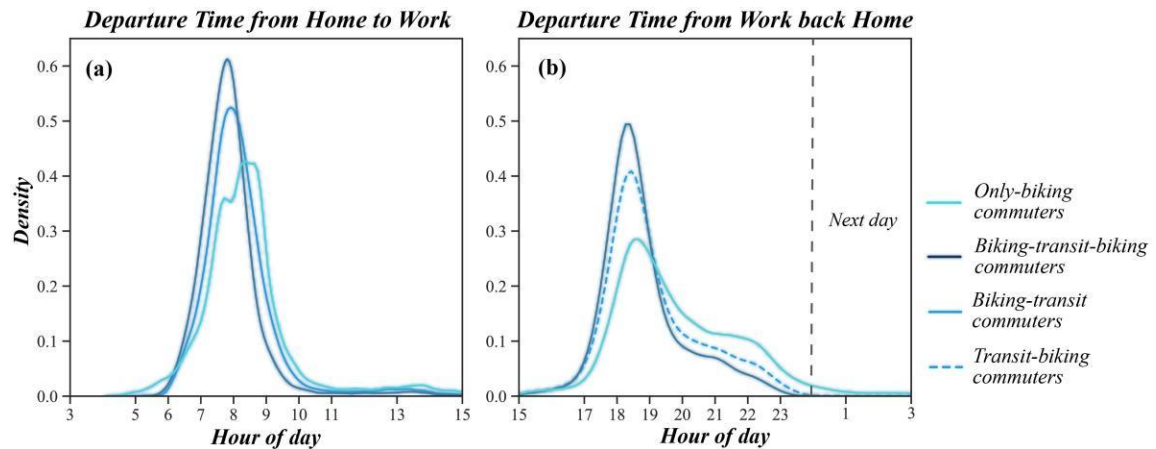


**Fig. 12** (a) Daily temporal patterns of commuting to work for *Only-biking*, *Biking-transit-biking* and *Biking-transit* commuters; (d) Daily temporal patterns of commuting home for *Only-biking*, *Biking-transit-biking* and *Transit-biking* commuters

#### 4.3.2 Spatial distribution of workplaces and residences for bike-sharing commuters

Fig.13(a) illustrates the density distribution of residential locations for all bike-sharing commuters, excluding *Transit-biking* commuters who cannot be identified to their residences. Likewise, Fig.13(b) shows the distribution of workplace for all commuters except for *Biking-transit* commuters. Generally, the spatial distributions of residential and employment area for bike-sharing commuters are similar, with widespread dispersion and local concentrations. Specifically, the employment hotspots are predominantly in the Futian FTZ – Futian CBD – Luohu CBD, High-tech Park – Bao'an Center and Longhua Industrial Park, with most residential hotspots distributed near these employment zones. This result is in line with the mixed land use patterns in Shenzhen. Interestingly, we discover that the main residential hotspots are in urban villages and old communities, especially in the central city. These areas

attract a large number of young migrants and graduates for rental housing due to the lower living cost (Liu et al. 2010). Concurrently, Guo et al. (2019) found that this demographic is also the main force of dockless bike-sharing users. Moreover, the narrow roads, high-density buildings, and mixed land use in these areas are more suitable for flexible and convenient bicycle trips. Thus, despite the difficulties of managing and dispatching bikes within complex urban villages and old communities, the substantial mobility demand (especially for commuting) in these areas still deserves the attention of bike-sharing operators.

Moreover, we calculate the average working hours in the major job centers in Shenzhen. It is worth noting that the calculated working hours are longer than the actual working hours for most users, as explained in Subsection 4.2.1, yet this discrepancy does not impede inter-regional comparison. The result shows that central city areas generally have shorter working hours than in the suburbs areas (Fig.13(b)). Specifically, in the central city, employment centers dominated by commercial and service industries (e.g., Luohu CBD and Futian CBD) exhibit shorter working hours compared to those focused on high-tech industries (e.g., High-tech Park). Notably, Huaqiang North Commercial Area has the shortest average working hours (9.89h). Conversely, in the suburbs, Longhua Industrial Park, which is mainly manufacturing, has the longest average working hours (10.89h), implying a higher likelihood of overtime for bike-sharing commuters employed here.

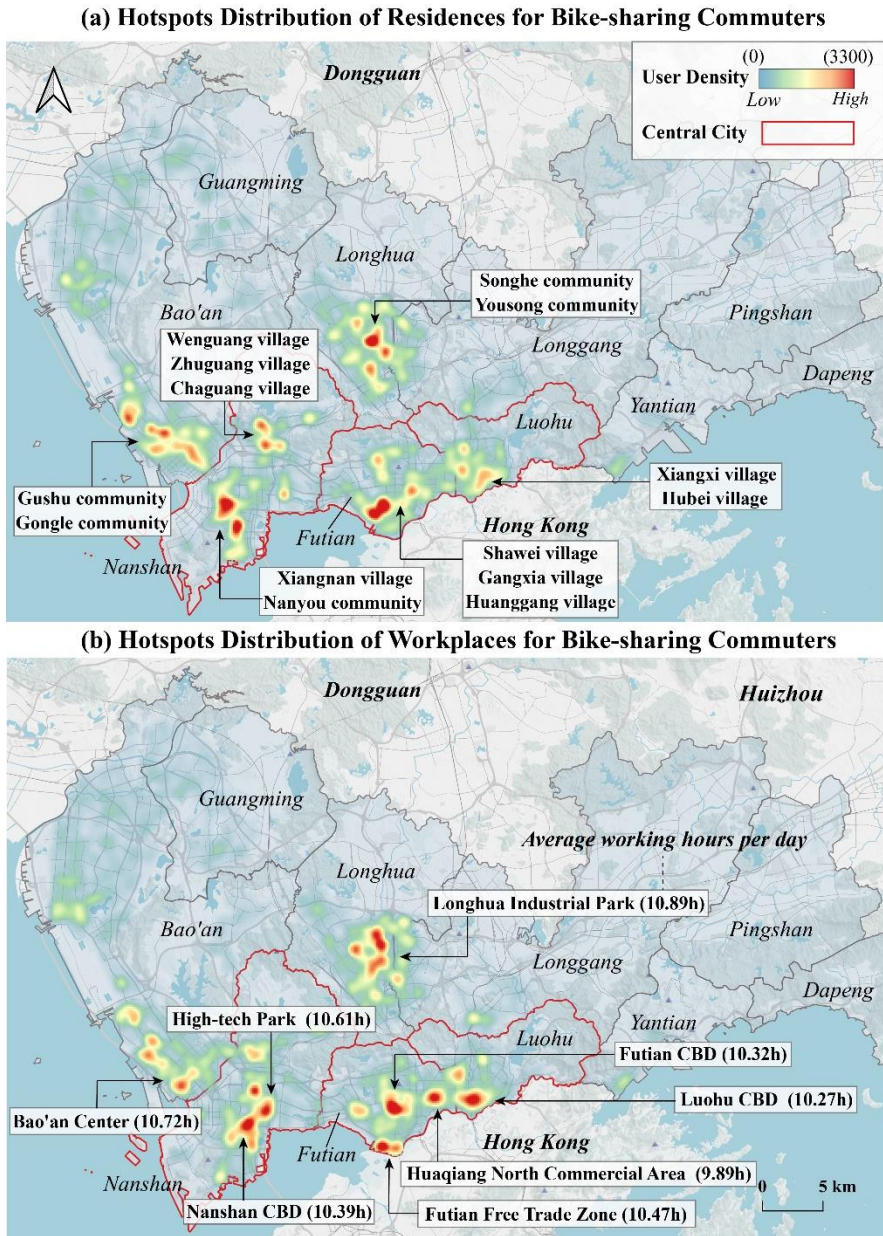


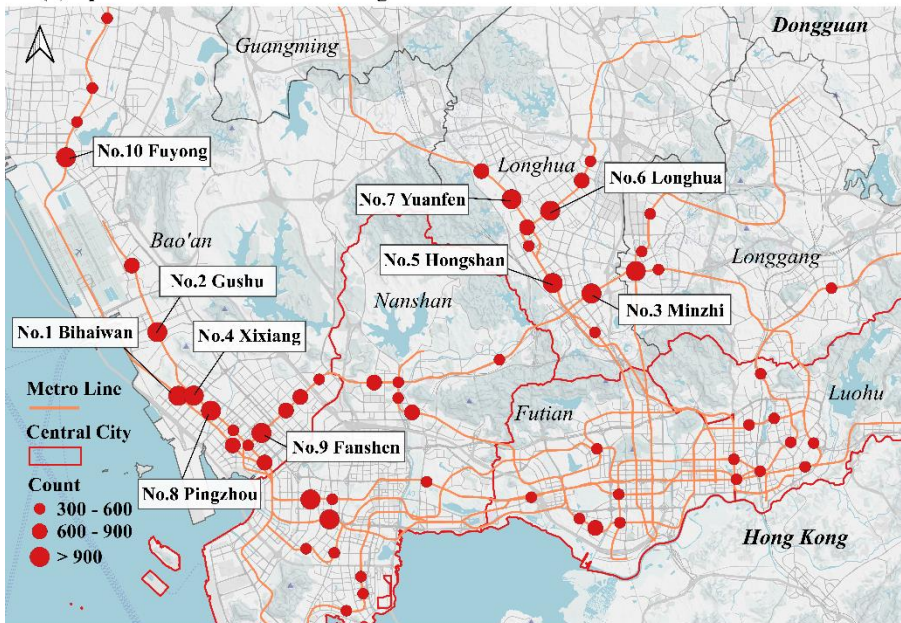
**Fig. 13** Hotspots distribution of residences and workplaces for bike-sharing commuters

#### 4.3.3 Spatial distribution of transfer stations for bike-sharing commuters

In Fig.14, we respectively aggregate *Biking-transit* and *Transit-biking* commuters by the metro stations they use daily, with the station size on the maps represents the number of bike-sharing commuters. Notably, Fig.14 also contains *Biking-transit-biking* commuters as

they have the characteristics of *Biking-transit* and *Transit-biking commuters*. For *Biking-transit commuters* (Fig.14(a)), while the spatial distribution of metro stations for them is similar to the residential hotspots in Fig.13(a), the metro stations with high cycling-transfer rate are mainly concentrated in the outskirts of the central city (e.g., Gushu, Minzhi, Hongshan, etc.). This result aligns with the finding of Guo et al. (2020), revealing the distribution of the main residences of groups use bike-sharing transfer services for across-district commuting. As for *Transit-biking commuters* (Fig.14(b)), most metro stations with high cycling-transfer rate are concentrated in central areas near mainly employment centers (especially Nanshan and Futian districts). However, only a few stations aggregate over 900 *Transit-biking commuters*. This is likely to the central area's high accessibility and proximity of businesses to metro stations (e.g., High-tech Park, Keyuan, etc.) facilitate direct walking to work, reducing the need for bike-sharing. Moreover, we observe that some metro stations (e.g., Bihaiwan, Gushu, Xili, etc.) have both lots of *Biking-transit* and *Transit-biking commuters*, which reflects a mixed use of living and working spaces. Thus, bike-sharing operators should pay attention to monitor the bicycle supply and demand around these stations.

(a) Spatial Distribution of *Biking-transit Commuters* at the Metro Station Level



(b) Spatial Distribution of *Transit-biking Commuters* at the Metro Station Level

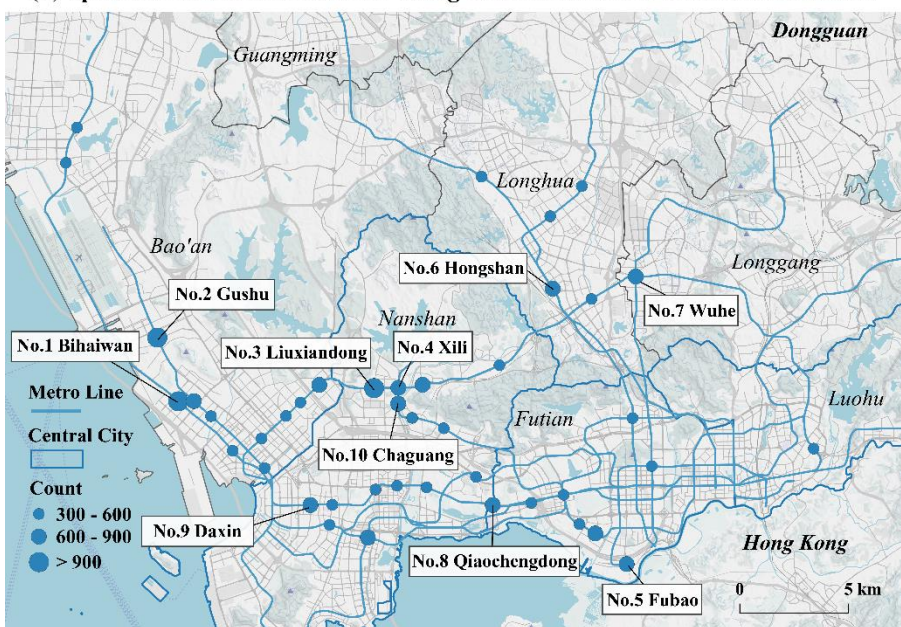


**Fig. 14** Spatial distribution of *Biking-with-transit commuters* at the metro station level

#### 4.3.4 Spatial patterns of bike-sharing users' commuting chains

To further insights into the commuting mobility of bike-sharing commuters, we analyze the biking commuting chains for *Only-biking* and *Biking-transit-biking commuters* by linking

their residences and workplaces to delineate their daily commuting flows, with residence as the origin and workplace as the destination. Utilizing the spatial clustering method by Gao et al. (2020), we present the results of primary commuting flow clusters in Fig. 15 and 16.

For *Only-biking commuters* (Fig.15), we discover that the commuting flow clusters are generally short in length, averaging 1.28 km, and regularly converge from the hotspots of residence to the nearest employment centers, in agreement with the observations in Fig. 10(b) and Fig.13. This result suggests that dockless bike-sharing play a significant role in short-distance commuting for residents in inner-city and suburban areas, further extending the findings of previous studies (Li et al., 2021; Gao et al., 2022). As for *Biking-transit-biking commuters* (Fig.16), the commuting flow clusters predominantly extend from the suburbs to the central city, with an average length of over 15 km. Specifically, these users mostly live in Bao'an and Longhua districts and daily commute by cycling to transfer with the metro that link the suburban and central areas (especially the Shenzhen Metro 1, 4, 5, and 11 Lines), echoing the actual situation in Shenzhen (e.g., many tech workers live near Pingzhou Station and work in the High-tech Park) and the analysis in Fig.14(a).

### Spatial Distribution of Commuting Flow Clusters for *Only-biking Commuters*

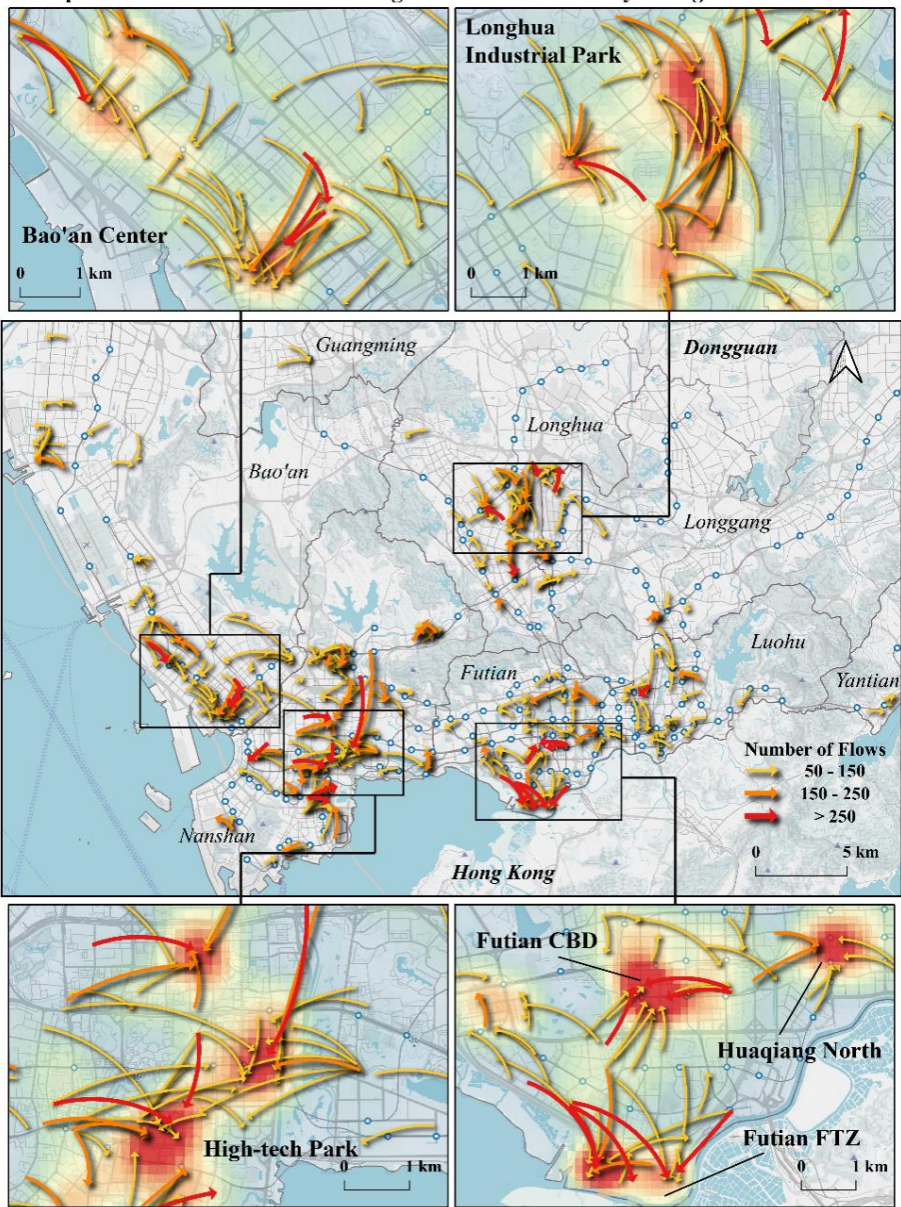


**Fig. 15** Spatial distribution of commuting flow clusters for *Only-biking commuters*

**Spatial Distribution of Commuting Flow Clusters for *Biking-transit-biking* Commuters**

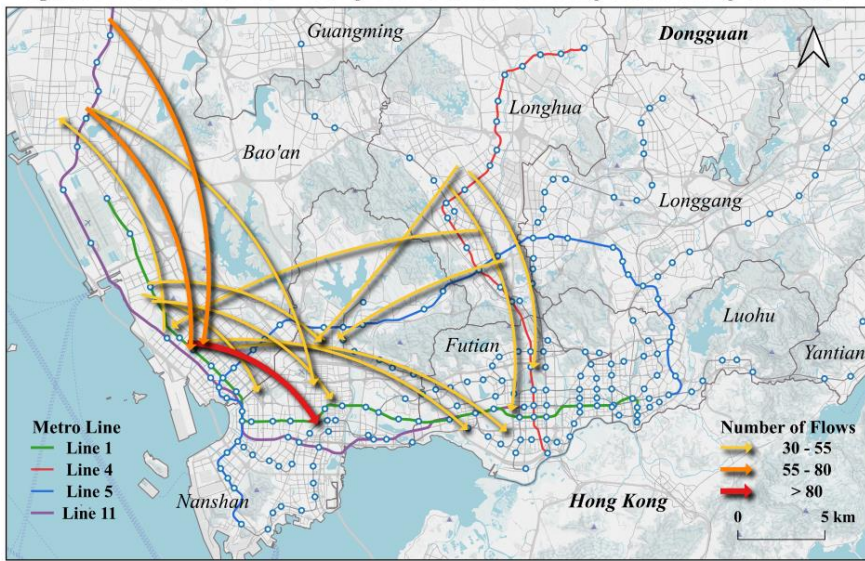


**Fig. 16** Spatial distribution of commuting flow clusters for *Biking-transit-biking* commuters

## 5 Conclusion

Mining individual daily travel patterns of bike-sharing users is vital for the increasingly refined planning of active transportation systems but remains a complex endeavor. To bridge this address, this paper presents a two-layer framework that integrates spatiotemporal flow clustering and rule-based decision trees, which is validated and applied to a dataset of over 200 million dockless bike-sharing trips in Shenzhen. In Layer 1, to overcome the lack of geocoding information in dockless bike-sharing trip data, we propose flow clustering methods with improved spatiotemporal constraints to identify users' daily trajectories from their disordered travel records, and confirm their performance through comparative analysis with the original methods. To the best of our knowledge, this is the first attempt to extract individual daily mobility using spatiotemporal flow clustering models, which can be extended to relevant studies on other travel data (e.g., taxi trip data). In Layer 2, considering

the characteristics of bicycle travels, we integrate round trip, working hours, and public transportation transfer to construct rule-based decision trees. These decision trees can identify the commuting behavior from users' daily cycling trajectories, thus deriving individual daily commuting patterns. Such information can assist urban planners and bike-sharing operators to rapidly understand residents' daily cycling patterns and demands. Moreover, it serves as a data foundation for fine-scale research on bicycle behavior by fusing multi-source data (e.g., street view images and housing prices).

Moreover, by applying the two-layer framework to the case study of Shenzhen, we have obtained some encouraging findings. First, the residential and workplace locations of bike-sharing commuters exhibit mixed distribution pattern of widespread dispersion with local concentrations. Most commuters live in the urban villages and old communities (especially in central city), while the residences of more *Biking-with-transit commuters* concentrate in the outskirts of the inner-city areas (e.g., near the Gushu and Hongshan Stations). Second, some bike-sharing users show noticeable overtime patterns, with a higher proportion of *Only-biking commuters* compared to *Biking-with-transit commuters*. In the mainly employment centers of the study area, Longhua Industrial Park, dominated by manufacturing, has the longest average working hours, exceeding 10 hours. Finally, we found that majority of active users utilize bike-sharing for commuting to work more frequently than for returning home, which is closely related to increased discretionary activities after work and the excessive bike-sharing demand around workplaces during commuting peak. These insights deepen our understanding of the daily mobility patterns of cycling community in megacities and provide decision-making support for the development of sustainable and human-oriented mobility,

ultimately contribute to increasing active transportation and improving public health.

However, there are still some limitations that warrant further improvement in future research. First, our framework limited to weekday commuting patterns of bike-sharing users, not accounting for weekend trips or non-commuting activities like exercise and leisure. Subsequent studies can leverage place data (e.g., Points of Interest) to explore the cycling characteristics in these contexts and develop more nuanced travel chain models. Second, it is necessary to validate mobility patterns with travel survey data, but regrettably, achieving this goal remains unattainable in our study due to the challenges in acquiring relevant data covering the study area's cycling population. Lastly, note that there is still a private bicycle (including electric bike) group in urban transportation. Investigating whether their mobility patterns resemble those of bike-sharing users is valuable, as it pertains to maximizing the benefits of building cycling-friendly environments.

## **6 Funding**

This study was supported by the National Science Fund for Distinguished Young Scholars (Grant No. 42225107), the National Natural Science Foundation of China (Grant No. 42271467).

## **7 References**

Cao, M., Huang, M., Ma, S., Lü, G., & Chen, M., 2020. Analysis of the spatiotemporal riding modes of dockless shared bicycles based on tensor decomposition. *Int. J. Geogr. Inf. Sci.* 34(11), 2225-2242.

Chen, W., Liu, X., Chen, X., Cheng, L., & Chen, J., 2023. Deciphering flow clusters from

large-scale free-floating bike sharing journey data: a two-stage flow clustering method. *Transportation*. 1-30.

Cheng, Z., Caverlee, J., Lee, K., & Sui, D., 2011. Exploring millions of footprints in location sharing services. In *Proceedings of the International AAAI Conference on Web and Social Media*. Vol. 5, No. 1, pp. 81-88.

Cheng, L., Mi, Z., Coffman, D. M., Meng, J., Liu, D., & Chang, D., 2021. The role of bike sharing in promoting transport resilience. *Netw. Spat. Econ.* 1-19.

Du, Y., Deng, F., Liao, F., 2019. A model framework for discovering the spatio-temporal usage patterns of public free-floating bike-sharing system. *Transp. Res. Part C Emerg. Technol.* 103, 39-55.

DeMaio, P., 2019. Bike-sharing: History, impacts, models of provision, and future. *J. Public. Trans.*, 12(4).

Ferretto, L., Bruzzone, F., & Nocera, S., 2021. Pathways to active mobility planning. *Research in transportation economics*, 86, 101027.

Fishman, E., 2016. Bikeshare: A review of recent literature. *Transp. Rev.* 36(1), 92-113.

Gao, X., Liu, Y., Yi, D., Qin, J., Qu, S., Huang, Y., & Zhang, J., 2020. A Spatial Flow Clustering Method Based on the Constraint of Origin-Destination Points' Location. *IEEE Access* 8, 216069-216082.

Gao, F., Li, S., Tan, Z., Wu, Z., Zhang, X., Huang, G., & Huang, Z., 2021a. Understanding the modifiable areal unit problem in dockless bike sharing usage and exploring the interactive effects of built environment factors. *Int. J. Geogr. Inf. Sci.* 35(9), 1905-1925.

Gao, K., Yang, Y., Li, A., Li, J., & Yu, B., 2021b. Quantifying economic benefits from free-

floating bike-sharing systems: a trip-level inference approach and city-scale analysis. *Transp. Res. A Policy Pract.* 144, 89-103.

Gao, F., Li, S., Tan, Z., & Liao, S., 2022. Visualizing the Spatiotemporal Characteristics of Dockless Bike Sharing Usage in Shenzhen, China. *J. Geovis. Spat. Anal.* 6(1), 1-15.

Gu, T., Kim, I., & Currie, G., 2019. To be or not to be dockless: Empirical analysis of dockless bikeshare development in China. *Transp. Res. A Policy Pract.* 119, 122-147.

Guangdong Statistics Bureau., 2021. Guangdong Statistical Yearbook 2021. Available at: <http://stats.gd.gov.cn/gdtjn/index.html>. (Accessed: 15 December 2023)

Guo, Y., & He, S. Y., 2020. Built environment effects on the integration of dockless bike-sharing and the metro. *Transp. Res. Part D: Transp. Environ.* 83, 102335.

Guo, Y., Yang, L., Lu, Y., & Zhao, R., 2021. Dockless bike-sharing as a feeder mode of metro commute? The role of the feeder-related built environment: Analytical framework and empirical evidence. *Sustain. Cities Soc.* 65, 102594.

Handy, S., Van Wee, B., & Kroesen, M., 2014. Promoting cycling for transport: research needs and challenges. *Transp. Rev.* 34(1), 4-24.

Heinen, E., Van Wee, B., & Maat, K., 2010. Commuting by bicycle: an overview of the literature. *Transp. Rev.* 30(1), 59-96.

Jiang, S., Ferreira, J., & Gonzalez, M. C., 2017. Activity-based human mobility patterns inferred from mobile phone data: A case study of Singapore. *IEEE Trans. Big Data* 3(2), 208-219.

Kim, K., 2023a. Investigation of modal integration of bike-sharing and public transit in Seoul for the holders of 365-day passes. *J. Transp. Geogr.* 106, 103518.

Kung, K. S., Greco, K., Sobolevsky, S., & Ratti, C., 2014. Exploring universal patterns in

human home-work commuting from mobile phone data. *PloS One* 9(6), e96180.

Li, S., Zhuang, C., Tan, Z., Gao, F., Lai, Z., & Wu, Z., 2021. Inferring the trip purposes and uncovering spatiotemporal activity patterns from dockless shared bike dataset in Shenzhen, China. *J. Transp. Geogr.* 91, 102974.

Li, L., Goodchild, M. F., & Xu, B., 2013. Spatial, temporal, and socioeconomic patterns in the use of Twitter and Flickr. *Cartogr. Geogr. Inf. Sci.* 40(2), 61-77.

Liu, Y., He, S., Wu, F., & Webster, C., 2010. Urban villages under China's rapid urbanization: Unregulated assets and transitional neighbourhoods. *Habitat Int.* 34(2), 135-144.

Liu, Y., Gao, X., Yi, D., Jiang, H., Zhao, Y., Xu, J., & Zhang, J., 2022. Investigating Human Travel Patterns from an Activity Semantic Flow Perspective: A Case Study within the Fifth Ring Road in Beijing Using Taxi Trajectory Data. *ISPRS Int. J. Geoinf.* 11(2), 140.

Liu, S., Zhang, X., Zhou, C., Rong, J., & Bian, Y., 2022. Temporal heterogeneous effects of land-use on dockless bike-sharing usage under transit-oriented development context: The case of Beijing. *J. Clean. Prod.* 380, 134917.

Liu, Y., Wang, S., Wang, X., Zheng, Y., Chen, X., Xu, Y., & Kang, C., 2024. Towards semantic enrichment for spatial interactions. *Ann. GIS.* 1-16.

Lu, Y., & Liu, Y., 2012. Pervasive location acquisition technologies: Opportunities and challenges for geospatial studies. *Comput. Environ. Urban. Syst.* 36(2), 105-108.

Luo, H., Kou, Z., Zhao, F., & Cai, H., 2019. Comparative life cycle assessment of station-based and dock-less bike sharing systems. *Resour. Conserv. Recycl.* 146, 180-189.

Ma, X., Ji, Y., Yang, M., Jin, Y., & Tan, X., 2018. Understanding bikeshare mode as a feeder to metro by isolating metro-bikeshare transfers from smart card data. *Transp. Policy* 71,

Ma, X., Ji, Y., Yuan, Y., Van Oort, N., Jin, Y., & Hoogendoorn, S., 2020. A comparison in travel patterns and determinants of user demand between docked and dockless bike-sharing systems using multi-sourced data. *Transp. Res. A Policy Pract.* 139, 148-173.

Reiss, S., & Bogenberger, K., 2016. Validation of a relocation strategy for Munich's bike sharing system. *Transportation Research Procedia*. 19, 341-349.

Ross-Perez, A., Walton, N., & Pinto, N., 2022. Identifying trip purpose from a dockless bike-sharing system in Manchester. *J. Transp. Geogr.* 99, 103293.

Sari Aslam, N., Cheng, T., & Cheshire, J., 2019. A high-precision heuristic model to detect home and work locations from smart card data. *Geo-Spat. Inf. Sci.* 22(1), 1-11.

Schwanen, T., & Dijst, M., 2002. Travel-time ratios for visits to the workplace: the relationship between commuting time and work duration. *Transp. Res. A Policy Pract.* 36(7), 573-592.

Shen, Y., Zhang, X., & Zhao, J., 2018. Understanding the usage of dockless bike sharing in Singapore. *Int. J. Sustain. Transp.* 12(9), 686-700.

Singleton, P. A., & Clifton, K. J., 2014. Exploring synergy in bicycle and transit use: Empirical evidence at two scales. *Transp. Res. Rec.* 2417(1), 92-102.

Si, H., Shi, J. G., Wu, G., Chen, J., & Zhao, X., 2019. Mapping the bike sharing research published from 2010 to 2018: A scientometric review. *J. Clean. Prod.* 213, 415-427.

Statistics Bureau of Shenzhen., 2022. Bike-sharing. Available at: [http://jtys.sz.gov.cn/zwgk/ztl/msss/2022gjcxxcz/jbqk/content/post\\_10150527.html](http://jtys.sz.gov.cn/zwgk/ztl/msss/2022gjcxxcz/jbqk/content/post_10150527.html) (Accessed: 15 December 2023)

Teixeira, J. F., Silva, C., & e Sá, F. M., 2021. The motivations for using bike sharing during

the COVID-19 pandemic: Insights from Lisbon. *Transport. Res. F Traf.* 82, 378-399.

Wu, M., Liu, X., Qin, Y., & Huang, Q., 2023. Revealing racial-ethnic segregation with individual experienced segregation indices based on social media data: A case study in Los Angeles-Long Beach-Anaheim. *Comput. Environ. Urban. Syst.* 104, 102008.

Xu, Y., Belyi, A., Bojic, I., & Ratti, C., 2018. Human mobility and socioeconomic status: Analysis of Singapore and Boston. *Comput. Environ. Urban. Syst.* 72, 51-67.

Xing, Y., Wang, K., & Lu, J. J., 2020. Exploring travel patterns and trip purposes of dockless bike-sharing by analyzing massive bike-sharing data in Shanghai, China. *J. Transp. Geogr.* 87, 102787.

Yao, X., Zhu, D., Gao, Y., Wu, L., Zhang, P., & Liu, Y., 2018. A stepwise spatiotemporal flow clustering method for discovering mobility trends. *IEEE Access* 6, 44666-44675.

Yao, Y., Jiang, X., & Li, Z., 2019. Spatiotemporal characteristics of green travel: A classification study on a public bicycle system. *J. Clean. Prod.* 238, 117892.

Yang, Y., Heppenstall, A., Turner, A., & Comber, A., 2019. A spatiotemporal and graph-based analysis of dockless bike sharing patterns to understand urban flows over the last mile. *Comput. Environ. Urban. Syst.* 77, 101361.

Yin, L., Lin, N., & Zhao, Z., 2021. Mining daily activity chains from large-scale mobile phone location data. *Cities*. 109, 103013.

Zhou, X., 2015. Understanding spatiotemporal patterns of biking behavior by analyzing massive bike sharing data in Chicago. *PLoS One.* 10(10), e0137922.

Zhang, Y., & Mi, Z., 2018. Environmental benefits of bike sharing: A big data-based analysis. *Appl. Energ.* 220, 296-301.

Zhang, Y., Aslam, N. S., Lai, J., & Cheng, T., 2020. You are how you travel: A multi-task learning framework for Geodemographic inference using transit smart card data. *Comput. Environ. Urban. Syst.* 83, 101517.

Zhang, H., Zhuge, C., Jia, J., Shi, B., & Wang, W., 2021a. Green travel mobility of dockless bike-sharing based on trip data in big cities: A spatial network analysis. *J. Clean. Prod.* 313, 127930.

Zhang, X., Shen, Y., & Zhao, J., 2021b. The mobility pattern of dockless bike sharing: A four-month study in Singapore. *Transp. Res. Part D: Transp. Environ.* 98, 102961.